ACCSCIENCE PUBLISHING

International Journal of Bioprinting

RESEARCH ARTICLE

Cell-laden hybrid gelatin–polyvinyl alcohol bioinks crosslinked with genipin for diabetic wound healing: A safety and efficacy analysis

Syafira Masri[1,2], Manira Maarof[1,3], Izhar Abd Aziz[4], and Mh Busra Fauzi[1,3]*

[1]Department of Tissue Engineering and Regenerative Medicine, Faculty of Medicine, Universiti Kebangsaan Malaysia, Cheras, Kuala Lumpur, Malaysia

[2]Department of Medical Informatics, RCSI & UCD Malaysia Campus (RUMC), George Town, Pulau Pinang, Malaysia

[3]Advance Bioactive Materials-Cells UKM Research Group, Universiti Kebangsaan Malaysia, Bangi, Selangor, Malaysia

[4]3D Gens Sdn Bhd, Bukit Jelutong, Shah Alam, Malaysia

Abstract

Three-dimensional (3D) bioprinting is an advanced tissue-engineering approach that utilises biomaterial-based bioinks to replace damaged skin and promote tissue regeneration. Compared with conventional skin grafting procedures, which are often painful and limited in treating extensive or irregular wounds, 3D-bioprinted constructs offer a more adaptable and minimally invasive alternative. Previously optimised biocompatible, biodegradable, and printable bioink formulations were further evaluated for skin regeneration using a diabetic mouse model of chronic wound healing from day 0 to day 17. Gelatin (GE) and polyvinyl alcohol (PVA) were formulated at different compositions (6% GE:0% PVA and 6% GE:5% PVA), with 0.1% genipin incorporated as a crosslinking agent to improve structural stability and printability. Assessment of PBMC metabolic activity supported the biocompatibility of the formulated hydrogels. In a full-thickness excisional wound model, bioink-treated groups exhibited accelerated wound closure, improved tissue organisation, and enhanced skin maturation compared with untreated controls. Furthermore, subcutaneous implantation studies revealed substantial hydrogel biodegradation within 14 days. Histological observations indicated the formation of skin microstructures resembling native tissue. Overall, these findings suggest that 3D-bioprinted GE–PVA hydrogels represent a promising strategy for promoting rapid, effective chronic wound healing and may serve as a potential alternative for future skin tissue-engineering applications.

Keywords: 3D-bioprinting; Chronic wound; Hydrogel; Gelatin–polyvinyl alcohol; Bioinks

***Corresponding author:**
Mh Busra Fauzi
(fauzibusra@ukm.edu.my)

Citation: Masri S, Maarof M, Aziz IA, Fauzi MB. Cell-laden hybrid gelatin–PVA bioinks crosslinked with genipin for diabetic wound healing: A safety and efficacy analysis. *Int J Bioprint*. 2026;12(5):026300313. doi: 10.36922/IJB026300313

Received: July 20, 2026

Revised: August 8, 2026

Accepted: August 13, 2026

Published online: September 10, 2026

Copyright: © 2026 Author(s). This is an Open-Access article distributed under the terms of the Creative Commons Attribution License, permitting distribution, and reproduction in any medium, provided the original work is properly cited.

Publisher's Note: AccScience Publishing remains neutral with regard to jurisdictional claims in published maps and institutional affiliations.

1. Introduction

A chronic wound is a type of wound that does not follow the usual healing process and does not go through the wound healing phases in an ordered and timely manner. This type of wound can last for a long time and be extremely painful. In most cases, the healing process for wounds consists of a series of steps, including hemostasis (blood

clotting), inflammation, proliferation (formation of new tissue), and remodelling (maturation of tissue).[1] When a person has a chronic wound, the natural healing process is impeded, leading to a prolonged healing time. Chronic wounds typically endure for extended periods, ranging from weeks to months or even years. Chronic wounds frequently produce exudate and may develop unpleasant odours. Without a complete skin barrier, these wounds are vulnerable to further injury and might increase in size.[2] The four primary categories of chronic wounds include pressure ulcers, diabetic foot ulcers (DFUs), venous ulcers, and arterial insufficiency ulcers. Inadequate glycaemic management leads to immunological dysfunction, resulting in reduced activity of white blood cells and decreased complement system function. This impaired immune response creates favourable conditions for the development of invasive tissue infections. The development of a foot ulcer in a person with diabetes is a serious complication that can lead to amputation if not treated promptly.

Thus, diverse wound dressings with intrinsic wound healing activity and/or bioactive compound release have been developed for the treatment of chronic wounds. Chronic wounds require many dressing changes, several hospitalisations, and physical restrictions.[3] These factors place a significant burden on patients and lower their quality of life. At a basic level, for chronic wounds, dressings should create a moist environment to minimise the likelihood of scar formation while promoting the growth of new skin cells and their migration into the wound. Gauze, sterile absorbent cotton, and dressings are frequently used in clinical practice because they are inexpensive and provide some physical protection for wounds.[4] However, dressing removal from the lesion may cause secondary tissue damage. As a result, the development of skin replacements offers several benefits over conventional dressings, especially in maintaining the moisture of the wound environment. In addition, skin substitute treatment helps prevent the recurrence of injury to newly formed granulation tissue caused by scarring and facilitates the growth, specialisation, and movement of skin cells.

At present, the global prevalence of DFUs ranges from 9.1 to 26.1 million cases per year, and the lifetime probability of having a DFU ranges from 19% to 34%.[5] Lower-extremity amputation is a common result of this chronic consequence of diabetes mellitus.[6] DFU is a condition characterised by discomfort, ulceration, and gangrene in the foot.[7] It is mostly caused by neuropathy and vascular disease affecting the lower extremities. The development of DFU is complicated, and its clinical symptoms vary widely. Prompt initiation of treatment is a crucial factor in achieving an excellent treatment outcome for DFU healing. In the field of tissue engineering, the increasing use of skin substitutes for the treatment of DFU can be attributed to their efficacy. Selection of the optimal biomaterial for skin substitutes is determined by criteria such as the nature and severity of the wound, as well as the wound's characteristics.[8]

The aim of employing skin substitutes is to mimic native skin while offering excellent biocompatibility and providing a platform for cell and growth factor loading to improve wound healing. Although skin grafts exhibit clinically acceptable biocompatibility, their application as an external material can lead to rejection by the body.[8] Thus, in tissue engineering, hydrogels are used as skin substitutes for chronic wound healing treatment due to their ability to retain oxygen, absorb wound exudate, and maintain a moist wound bed environment, making them ideal for DFU dressing development.[9] Hydrogels, which are three-dimensional (3D) networks of hydrophilic polymer chains, have the capacity to absorb water up to 10 times their original weight. Hydrogels' ability to provide a moist environment and serve as cell carriers has been shown to have beneficial effects on wound healing.[10]

In general, 3D-bioprinting is used to develop skin substitutes by encapsulating skin cells and biomaterials to generate the bioinks. Three-dimensional bioprinting enables precise control over cell distribution within 3D structures, promoting interactions between cells and the surrounding matrix.[11] Compared with conventional scaffold-based approaches, 3D bioprinting enables the controlled, layer-by-layer deposition of living cells and biomaterials, thereby allowing the fabrication of complex, biomimetic tissue constructs with improved spatial organisation.[12] This capability is particularly relevant for localised skin injuries, where precise placement of cells and biomaterials can facilitate tissue-specific regeneration and restoration of wound architecture.[12]

In addition, over the last five years, *in situ*-forming hydrogels and injectable systems have been investigated extensively as strategies for wound repair and regeneration. These approaches are relatively easy to apply and may conform closely to irregular wound defects without requiring additional adhesive or sutures because gels adhere to the precise shape of wound defects.[13] In a previous study, the efficacy of a cell-based ovine tendon collagen type I scaffold incorporating human skin cells was compared with that of the cell-free scaffold in treating nude mice.[14] It was shown that the incorporation of skin cells into the scaffold facilitated the healing progress *in vitro* and *in vivo*. Despite the efficacy of these approaches, hydrogels may be particularly suitable for DFU treatment

because of their moisture-retention properties.

This study aimed to investigate the safety and efficacy of a gelatin (GE)–polyvinyl alcohol (PVA) hydrogel crosslinked with genipin (GNP) as a bioink (cellular treatment) and an injectable hydrogel (acellular treatment) for DFU. As part of a continuous study, the physicochemical, rheological, mechanical, printability, and *in vitro* biocompatibility characteristics of the GE–PVA/GNP bioinks have been comprehensively investigated in our previous studies using primary human dermal fibroblasts.[1,15,16] The studies have established the suitability of the optimised formulations, namely the gelatin–genipin (GE_GNP) bioink, gelatin with 5% poly(vinyl alcohol) and genipin (GPVA5_GNP) bioink, GE_GNP injectable hydrogel, and GPVA5_GNP injectable hydrogel, for wound-healing applications. The optimised formulations exhibited increased viscosity, complex viscosity, storage modulus (G′), and loss modulus (G″), together with shear-thinning behaviour, which contributed to improved filament formation, print fidelity, and structural stability during extrusion-based bioprinting. Based on these findings, the optimised GE_GNP and GPVA5_GNP formulations were selected for the subsequent *in vivo* evaluation.

Building upon these findings, the present study focuses on the subsequent *in vivo* evaluation of these optimised formulations as immediate treatments for chronic wounds in a diabetic mouse model (within 6 to 8 h post-biopsy). In addition, the metabolic activity of peripheral blood mononuclear cells (PBMCs) following exposure to the formulations was investigated *in vitro* to complement the biological safety evaluation and therapeutic potential of the developed hydrogels for DFU management.

2. Materials and methods

2.1. Preparation of sterile gelatin-polyvinyl alcohol bioinks

Briefly, sterile PVA solutions (3% and 5%, w/v) were prepared by dissolving partially hydrolysed PVA (≥85%; molecular weight 70,000 g/mol; Merck KGaA, Germany) in distilled water at 60 °C. Sterile gelatin (Nitta Gelatin Inc., Japan) was subsequently added to the PVA solutions at 40 °C to obtain homogeneous GE–PVA formulations containing 6% (w/v) gelatin. Genipin (FUJIFILM Wako Pure Chemical Corporation, Japan) was dissolved in 70% ethanol (Merck KGaA, Germany) and incorporated into the homogeneous GE–PVA formulations at a final concentration of 0.1% (w/v) to facilitate hydrogel crosslinking. The resulting formulations were used for the preparation of injectable hydrogels and 3D-bioprinted constructs.

For 3D bioprinting, the sterile bioinks were loaded into sterile printing syringes fitted with a nozzle having an inner diameter of 0.3 mm, and the constructs were fabricated using an extrusion-based 3D bioprinter (Biogens XI, 3D Gens, Malaysia). Each bioink was extruded through the nozzle layer by layer to produce the desired hydrogel constructs. The resulting injectable and 3D-bioprinted hydrogels were subsequently used for further characterisation and evaluation.

2.2. Study approval

The study design was approved by the Universiti Kebangsaan Malaysia Research Ethics Committee (code nos. FF-2021-376 and JEP-2021-605) and Universiti Kebangsaan Malaysia Animal Ethic Committee (UKMAEC) (code nos. TEC/FP/2023/MOHD FAUZI/26-JULY/1356-SEPT.-2023-SEPT.-2025 and FF-2023-284). The research was performed in certified facilities under an ISO 9001:2015 quality management system.

2.3. Metabolic activity of peripheral blood mononuclear cells exposed to gelatin–polyvinyl alcohol hydrogels

Heparinised vacutainers (13 × 75 mm, 4 mL; Becton Dickinson, United States of America [USA]) were used to collect PBMCs from six healthy volunteers. After blood collection, the vacutainers were then centrifuged at 400 × g for 30 min over a Ficoll–Paque density gradient to isolate the cells. The cells were subsequently suspended in culture medium (RPMI-1640 medium, supplemented with 2 mM L-glutamine [Gibco, USA], 100 U/mL penicillin and 100 μg/mL streptomycin [Invitrogen, USA], and 10% fetal bovine serum [Capricorn Scientific GmbH, Germany]) and seeded at a density of 1.0×10^6 cells per well in a 96-well plate, with each well containing 100 μL of culture medium. Following that, the cells were layered with a hydrogel disc and incubated in a 96-well plate for 6 days. The PBMCs suspended in culture medium served as the negative control, whereas PBMCs treated with phytohemagglutinin (PHA) (Roche, Merck, USA) served as the positive control. The treatment groups were exposed to GE_GNP or GPVA5_GNP hydrogel discs. Cell viability was assessed using the 3-(4,5-dimethylthiazol-2-yl)-2,5-diphenyl-2H-tetrazolium bromide (MTT) assay (Invitrogen, Thermo Fisher Scientific, USA) on days 1, 3, and 6. The cells were incubated with MTT reagent (final concentration: 5 μg/mL) for 4 h at 37 °C The formazan, used as an indicator of cell viability, was dissolved by adding 100 μL of dimethyl sulfoxide to each well and incubating for 10 min. Finally, a PowerWave XS microplate reader (BioTek Instruments, Inc., USA) was used to determine the optical absorbance of the supernatants at 570 nm.

2.4. Induction of type I diabetes mellitus in mouse model

A total of 36 male C57BL/6 mice, aged 8 weeks and weighing between 20 g and 30 g, were used in the diabetic wound-healing experiment. The mice were obtained from Labrat Breeders Farm, Malaysia, and six mice were allocated to each of the six experimental groups ($n = 6$ per group). They were placed in individually ventilated cages (194 mm × 182 mm × 394 mm), acclimatised to the laboratory environment under a 12-h light/dark cycle for one week, and given access to food (Altromin #1324 Diet, Germany) and autoclaved water. After acclimatisation, food and water were removed from the cages 4 h before streptozotocin (STZ; ≥97%; Thermo Scientific Chemicals, USA) injection. Then, 4 mg of STZ was weighed into a 1.5-mL microcentrifuge tube covered with aluminium foil, with one tube prepared for every three mice. The STZ was dissolved in 50 mM sodium citrate buffer (pH 4.5) before injection, resulting in a final concentration of 4 mg/mL. The experimental-group mice were injected intraperitoneally (i.p.) with STZ at 40 mg/kg (1.0 mL/100 g) using 1-mL syringes and 27G needles.[17] The STZ injection was repeated daily for the following 4 days. After injection, the mice were placed back in their cages with access to food and 10% sucrose water.

The catabolic consequences of insulin insufficiency and severe hyperglycaemia, together with volume loss associated with osmotic diuresis, may contribute to significant weight loss in later-stage STZ-induced diabetic mice. On day 6, the 10% sucrose water was replaced with normal autoclaved water. To confirm hyperglycemia, the mice were fasted for 6 h on day 9 after STZ injection, and a tail-vein blood sample was then analysed using an Accu-Chek blood glucose monitoring system (Roche Diabetes Care, Switzerland). The STZ-treated mice were classified as diabetic if their blood glucose levels exceeded 11.7 mmol/L (300 mg/dL).[18] However, mice with blood glucose levels below the threshold of 11.7 mmol/L were administered an additional STZ dose of 200 mg/kg.[18] The diabetic mice in the treatment group received the scaffold, whereas the diabetic control mice received normal saline.

2.5. *In vivo* model for treatment of chronic wounds in diabetic mice

The diabetic mice were anaesthetised by intramuscular administration of a combination of ketamine (5.6 mg/kg; Ketamav 50, Mavlab, Australia), xylazil-100 (5.6 mg/kg; Troy Laboratories, Australia), and tiletamine (2.8 mg/kg; Zolatil 20, Virbac Laboratories, France) prior to wound creation. Before administration, the anaesthetic cocktail was diluted with water for injection at a ratio of 1:4. An alcohol swab was used to clean the hind legs of the mice, and surgical scissors were used to create a full-thickness circular skin wound with a diameter of 1 cm (surface area, 0.785 cm^2). The excised 1-cm-diameter skin specimens were then digested with 0.6% collagenase type I (Worthington, USA) to obtain cells for bioink formulation. After enzymatic digestion, the skin tissues were trypsinised using trypsin–EDTA (Gibco, USA) and washed with Dulbecco's phosphate-buffered saline (Gibco, Thermo Fisher Scientific, USA). Sterile hydrogel solutions were then mixed with the isolated mouse skin cells to obtain GE_GNP and GPVA5_GNP bioinks, which were subsequently printed to produce hydrogel constructs.

The cell-laden bioinks were fabricated using an extrusion-based 3D bioprinter equipped with a sterile printing syringe with an inner diameter of 0.3 mm. Bioprinting was performed at a printing speed of 4,000 mm/s and a printing temperature ranging from 19–27 °C, depending on the formulation, to fabricate hydrogel constructs with a diameter of 1 cm and a thickness of 0.5 mm. The bioinks contained 0.1% (w/v) *GNP* (FUJIFILM Wako Pure Chemical Corporation, Japan) as a chemical crosslinking agent to improve the structural stability of the printed constructs. The optimisation of the printing parameters was described in our previous studies.[1,16] In addition, other treatment groups received cell-free injectable hydrogels applied to the 1-cm-diameter wound, constituting the GE_GNP inj and GPVA5_GNP inj groups. Integra, a commercial wound dressing (Integra LifeSciences Corporation, USA), was also used in another treatment group.

For the control groups, 10 μL of normal saline was applied to the wound. To prevent displacement of the scaffolds after implantation, the hydrogels were layered with Otosilk (P & L Medical (M) Sdn. Bhd., Malaysia) and sutured at six locations. The wounds were covered with sterile gauze and secured with Hypafix adhesive tape (BSN Medical, Germany). The wound dressings were replaced on day 7 after implantation. Wound healing was evaluated by analysing the gross appearance of the wounds using a standard digital camera on days 0, 7, 14, and 17. The epidermal and dermal layers of the regenerated skin were measured at 10 distinct points for each layer per sample using ImageJ software (version V1.5, Bethesda, USA). Figure 1 shows the different treatment groups in the diabetic wound model.

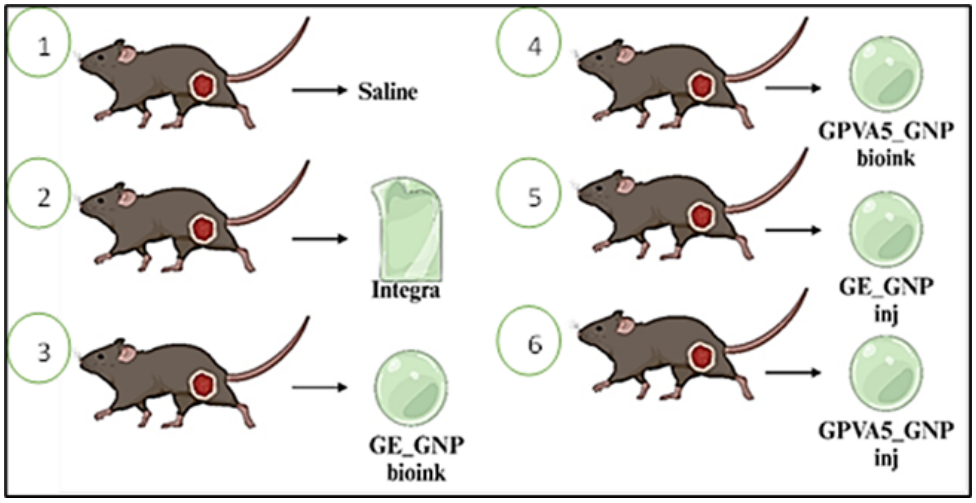

Figure 1. Illustration of diabetic mice with wounds assigned to the following treatment groups: saline, Integra, GE_GNP bioink, GPVA5_GNP bioink, GE_GNP inj, and GPVA5_GNP inj. Created in BioRender

2.6. *In vivo* model of subcutaneous hydrogel biodegradation

Prior to subcutaneous implantation of the hydrogels, the diabetic mice were anaesthetised by intramuscular administration of the same anaesthetic cocktail used in Section 2.5. A small incision (<1 cm long) was made in the dorsal region, and subcutaneous pockets were created using surgical scissors. Sterile hydrogel pieces (diameter: 1 cm; thickness: 0.4 cm) were then inserted into the subcutaneous pockets in the lower backs of the mice. The incisions were closed with absorbable sutures. To quantify *in vivo* biodegradation, the thickness of the implanted hydrogels was assessed on days 0, 7, and 14. On day 14, skin tissue surrounding the subcutaneous pockets was collected and preserved in formalin for histological examination. The percentage of *in vivo* biodegradation was calculated using **Equation 1**:

$$\text{Biodegradation}(\%) = \frac{(W1 - W2)}{W1} \times 100 \quad (1)$$

where W2 is the final hydrogel thickness and W1 is the initial hydrogel thickness.

2.7. Histological analysis of regenerated skin

Skin specimens (1 cm in diameter) were excised from euthanised diabetic mice and preserved in 10% buffered formalin (Sigma, USA) for histological analysis of wound regeneration. For histological staining, the samples were processed, embedded in paraffin, and sectioned at a thickness of 5 μm using a microtome (Leica, Germany). Hematoxylin and eosin (H&E; IHC World, USA), Masson's trichrome stain kit (Abcam, USA), and picrosirius red (Polysciences, USA) were used to visualise skin architecture, collagen deposition, and collagen types I and III, respectively. These staining methods enabled visualisation of cell nuclei and extracellular matrix components, allowing assessment of the structural characteristics of the epidermal and dermal layers.

Briefly, the paraffin-embedded skin sections were treated with xylene for deparaffinisation and gradually rehydrated using 100%, 95%, and 70% ethanol. The samples were then stained with H&E. Masson's trichrome staining was used to label collagen in blue and cell cytoplasm, keratin, muscle fibres, and erythrocytes in red. The tissue sections were deparaffinised and placed in preheated Bouin's fluid (56–64 °C) for 60 min and then allowed to cool for 10 min, as recommended by the manufacturer's protocol. After washing with running tap water, the slides were incubated with Weigert's iron hematoxylin for 5 min and washed with running tap water. The slides were then incubated with Biebrich scarlet/acid fuchsin solution for 15 min. After washing with running tap water, the slides were differentiated in phosphomolybdic/phosphotungstic acid solution for 10–15 min and washed with running tap water. The slides were then incubated with aniline blue solution for 5–10 min and washed with running tap water. The treated tissue sections were placed in acetic acid for 5 min, rinsed, dehydrated through a series of ethanol solutions, and cleared in xylene before mounting with dibutylphthalate polystyrene xylene (DPX) (Sigma-Aldrich, USA).

Picrosirius red staining was used to identify collagen, which appeared red, whereas muscle fibres and cytoplasm appeared yellow. The tissue sections were deparaffinised and

sequentially immersed in solution A (phosphomolybdic acid hydrate) for 2 min, solution B (2,4,6-trinitrophenol) for 60 min, and solution C (0.1% hydrochloric acid) for 2 min. Finally, the tissue sections were immersed in 70% ethanol for 45 s and then dehydrated through a series of ethanol solutions. Subsequently, the tissue sections were cleared in xylene and mounted with DPX. The collagen fibrils were observed using light microscopy (A1R-A1, Nikon, Japan).

2.8. Immunofluorescence analysis of regenerated skin

Immunofluorescence labelling was performed using primary antibodies against involucrin (Abcam, USA) and cytokeratin 14 (CK14; Abcam, USA) to examine epidermal marker expression. To evaluate dermal layer maturation, primary antibodies against collagen type I (Abcam, USA) and alpha-smooth muscle actin (α-SMA; Abcam) were used. The regenerated skin tissues were fixed in formalin and embedded in paraffin. Tissue sections with a thickness of 5 μm were prepared using a microtome. The sections were treated with xylene to remove the paraffin and then rehydrated through a graded series of ethanol solutions. The tissue sections were treated with an antigen retrieval solution (Sigma-Aldrich, USA). The sections were then incubated with 10% goat serum (Capricorn Scientific GmbH, Germany) at 37 °C for 1 h to block nonspecific binding sites. Subsequently, the tissue sections were incubated overnight with the primary antibodies at 4 °C. After washing with phosphate-buffered saline, the tissue sections were incubated with the secondary antibodies. The antibodies used were listed in Table 1.

The sections were subsequently counterstained with DAPI (Invitrogen, USA). Images were captured using a fluorescence microscope (A1R-A1, Nikon, Japan) at 100× magnification.

Table 1. Antibodies used for immunofluorescence staining

Skin layers	Targeted tissue/cell	Primary antibody	Secondary antibody
Epidermis layer	Skin keratinocytes/ cytokeratin	Rabbit anti-cytokeratin 14; dilution, 1:1,000	Goat anti-rabbit Alexa Fluor 594 (red); dilution, 1:1,000
	Stratum corneum	Rabbit anti-involucrin, concentration: 10 μg/mL	Goat anti-rabbit Alexa Fluor 594 (red); dilution, 1:1,000
Dermal layer	Skin fibroblasts	Rabbit anti-collagen type I; dilution, 1:1,000	Goat anti-rabbit Alexa Fluor 594 (red); dilution, 1:1,000
	Myofibroblasts	Rabbit anti-alpha smooth muscle actin; dilution, 1:1,000	Goat anti-rabbit Alexa Fluor 594 (red); dilution, 1:1,000

2.9. Evaluation of maturity of regenerated skin

Transmission electron microscopy (TEM) was used to assess the microscopic structure of regenerated skin, specifically the tight junction components, dermal–epidermal junction (DEJ), and collagen fibre formation, to assess the degree of skin maturity. The biopsies were sectioned into 0.5 × 0.5 mm pieces (0.5 mm^3) and fixed in 4% glutaraldehyde (Bio-Rad, USA) overnight at 4 °C. The samples were then washed with 0.1 M sodium cacodylate (Sigma-Aldrich, USA) and treated with 4% osmium tetroxide (Sigma-Aldrich, USA) for 1 h. They were again rinsed with sodium cacodylate and then dehydrated using a graded series of acetone solutions (Sigma-Aldrich, USA) ranging from 35% to 100%. Infiltration was performed using mixtures of acetone and resin at ratios of 1:1 for 1 h and 1:2 for 2 h, followed by 100% resin overnight. Polymerisation was then performed in an oven at 60 °C for 24–48 h. The samples were subsequently sectioned at a thickness of 90 nm using an ultramicrotome (Leica, Germany). Finally, the ultrathin sections were stained with lead citrate and uranyl acetate and examined using a TEM (Tecnai G2 Spirit BioTwin, FEI, USA).

2.10. Statistical analysis

All reported data were analysed using GraphPad Prism (V9.0, GraphPad Software Inc., USA). One-way and two-way ANOVA were used for multiple-group analysis. Data were expressed as the mean ± standard deviation. A p-value < 0.05 was considered statistically significant. All quantitative data were obtained from three replicate trials ($n = 3$).

3. Results

3.1. Peripheral blood mononuclear cell metabolic activity in response to bioinks and injectable hydrogels

The PBMCs were cultured in the presence of the hydrogels for up to 6 days, and their metabolic activity was assessed

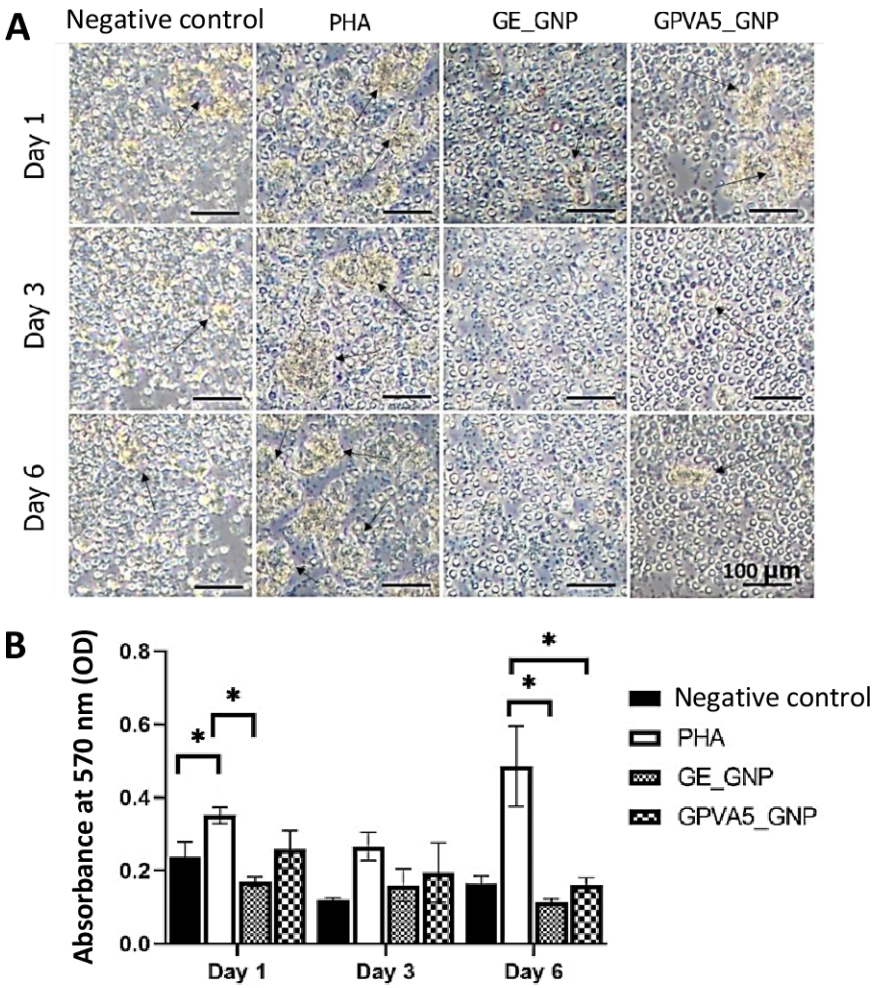

Figure 2. Safety assessment of hydrogels using peripheral blood mononuclear cells (PBMCs). (A) PBMC responses to the hydrogels on days 1, 3, and 6. PBMC clumping is indicated by black arrows. (B) Quantitative analysis of PBMC metabolic activity using the MTT assay. $^{*}p < 0.05$. Scale bars: 100 µm; magnification: 100×.

on days 1, 3, and 6. PBMC clumping in response to the treatments is shown in Figure 2A. PBMC clumping was observed in the PHA-treated control group from day 1 to day 6. In contrast, PBMC clumping decreased after 3 days of exposure to GE_GNP and GPVA5_GNP. Based on the quantitative data shown in Figure 2B, PBMCs treated with PHA showed an increase in metabolic activity from day 1 (0.351 ± 0.022 OD units) to day 6 (0.486 ± 0.110 OD units). The metabolic activity of PBMCs exposed to GE_GNP and GPVA5_GNP was 0.170 ± 0.014 OD units and 0.259 ± 0.051 OD units, respectively, on day 1. However, metabolic activity gradually decreased on day 3 (0.160 ± 0.045 OD units and 0.195 ± 0.081 OD units, respectively) and further decreased on day 6 (0.114 ± 0.011 OD units and 0.161 ± 0.021 OD units, respectively).

3.2. Assessment of wound closure

Photographic monitoring of wound repair began on day 0 (the day of surgery) and continued until sacrifice ($n = 6$). Wound repair was evaluated by measuring the wound area defined by the re-epithelialisation boundaries at various time points during the study. During gross monitoring, the wounds treated with saline, Integra, injectable hydrogels (GE_GNP inj and GPVA5_GNP inj), or bioinks (GE_GNP bioink and GPVA5_GNP bioink) remained clean and dry with minimal exudate. As shown in Figure 3A, there was no significant difference in wound area on day 7 among wounds treated with saline, Integra, injectable hydrogels, and bioinks. However, from day 14 onward, a significant reduction in wound area compared with day 0 was observed in the Integra, bioink (GE_GNP bioink

and GPVA5_GNP bioink), and injectable hydrogel (GE_GNP inj and GPVA5_GNP inj) groups. Moreover, the GPVA5_GNP bioink group showed significantly greater wound closure on days 14 and 17, with no obvious scars, compared with the other treatment groups. Figure 3B shows the wound closure (%) in diabetic mice on days 0, 7, 14, and 17. On days 7, 14, and 17, the saline group showed wound closure rates of 48.64 ± 16.41%, 57.21 ± 12.81%, and 85.35 ± 1.98%, respectively.

The GPVA5_GNP bioink group showed the greatest wound closure, with closure rates of 82.41 ± 10.91%, 97.55 ± 1.77%, and 100% on days 7, 14, and 17, respectively, followed by the GE_GNP bioink group (73.14 ± 3.91%, 82.76 ± 19.27%, and 100%, respectively). The Integra group showed slower wound closure (73.09 ± 9.09%, 73.35 ± 20.24%, and 89.61 ± 2.77% on days 7, 14, and 17, respectively) compared with the bioink groups. The GE_GNP inj group showed wound closure rates of 76.81 ± 2.12%, 78.63 ± 2.96%, and 93.87 ± 3.55% on days 7, 14, and 17, respectively, whereas the GPVA5_GNP inj group showed corresponding rates of 68.12 ± 19.52%, 81.78 ± 8.31%, and 95.14 ± 1.64%).

3.3. Histological assessment of granulation tissue formation and dermal regeneration during diabetic wound healing in mice

Hematoxylin and eosin staining is a widely used histological method. In H&E staining, hematoxylin stains cell nuclei blue-purple, whereas eosin stains the cytoplasm and extracellular structures pink. As shown in Figure 4A, H&E staining revealed that the wounds in all groups had re-epithelialised by day 17. However, crusts or scabs remained in the saline and injectable hydrogel groups (GE_GNP inj and GPVA5_GNP inj), indicating that wound healing was still ongoing. The bioink groups showed re-epithelisation of the wounds, with a thin epidermal layer compared with the other treatment groups. The saline and Integra groups showed signs of inflammation, with an immature epidermis and thick crusts/scabs. The epidermis exhibited increased thickness and a stratified structure, whereas the dermal tissue remained moderately disorganised.

During the wound-healing process, the thickness of the epidermal layer in mouse skin wounds differed among the experimental groups on day 17. As shown in Figure 4B, the epidermal thickness of normal mouse skin was 30.90 ± 16.27 μm, whereas the saline group had the thickest epidermal layer (90.77 ± 32.37 μm). Both bioink-treated groups, GE_GNP bioink and GPVA5_GNP bioink, showed epidermal thicknesses close to that of normal skin (27.02 ± 11.15 μm and 31.26 ± 12.95 μm, respectively), compared with the GE_GNP inj, GPVA5_GNP inj, and Integra groups (57.19 ± 9.42 μm, 47.53 ± 18.59 μm, and 50.70 ± 15.80 μm, respectively). However, all experimental wound groups appeared to show greater dermal cellularity than normal skin, indicating that the remodelling phase of wound healing had not been fully completed. As shown in Figure 4C, dermal thickness was lower in all experimental wound groups than in normal mouse skin (463.55 ± 35.21 μm). The GE_GNP and GPVA5_GNP bioink groups, which contained encapsulated skin cells, demonstrated dermal thicknesses of 371.21 ± 49.27 μm and 331.96 ± 53.68 μm, respectively; both values were lower than that of normal skin. The saline group had a dermal thickness of 423.36 ± 66.27 μm, which was comparable to that of normal skin. Nevertheless, its dermal structure was loosely packed and disorganised.

Histopathological assessment of the skin tissues surrounding the implanted bioinks and injectable hydrogels was performed to evaluate *in vivo* biocompatibility, while changes in hydrogel thickness were monitored to assess *in vivo* degradation. The volume of the hydrogels gradually decreased over time. This degradation may be associated with the activity of endogenous enzymes, such as lipases, collagenases, proteases, and lysozyme.

Figure 5C illustrates the results of H&E staining of the skin tissue surrounding the hydrogels on day 14 after subcutaneous implantation. Numerous spindle-shaped cells and other infiltrating cells were observed at the implantation site, suggesting that the hydrogels may support fibroblast infiltration and granulation tissue formation. Inflammatory cells and fibroblasts were also observed around the hydrogels, consistent with an ongoing tissue response. Moreover, according to the quantitative biodegradation data in Figure 5B, the biodegradation rates of the GE_GNP and GPVA5_GNP bioinks from day 7 to day 14 were 23.68 ± 0.25% and 30.37± 4.96%, respectively. On day 14, the biodegradation rates of the GE_GNP and GPVA5_GNP injectable hydrogels were 29.40 ± 5.27% and 37.21 ± 0.93%, respectively.

3.4. Histological analysis of collagen matrix production in diabetic wound healing mice

Masson's trichrome staining is widely used to visualise collagen deposition in skin tissue during wound healing. Collagen, an essential component of the extracellular matrix, provides structural support to regenerating tissue. In Masson's trichrome staining, collagen fibres are typically stained blue or green, facilitating assessment of collagen deposition in skin tissue. As shown in Figure 6A, the morphology of the treated wound areas appeared improved in the treatment groups (bioinks, injectable

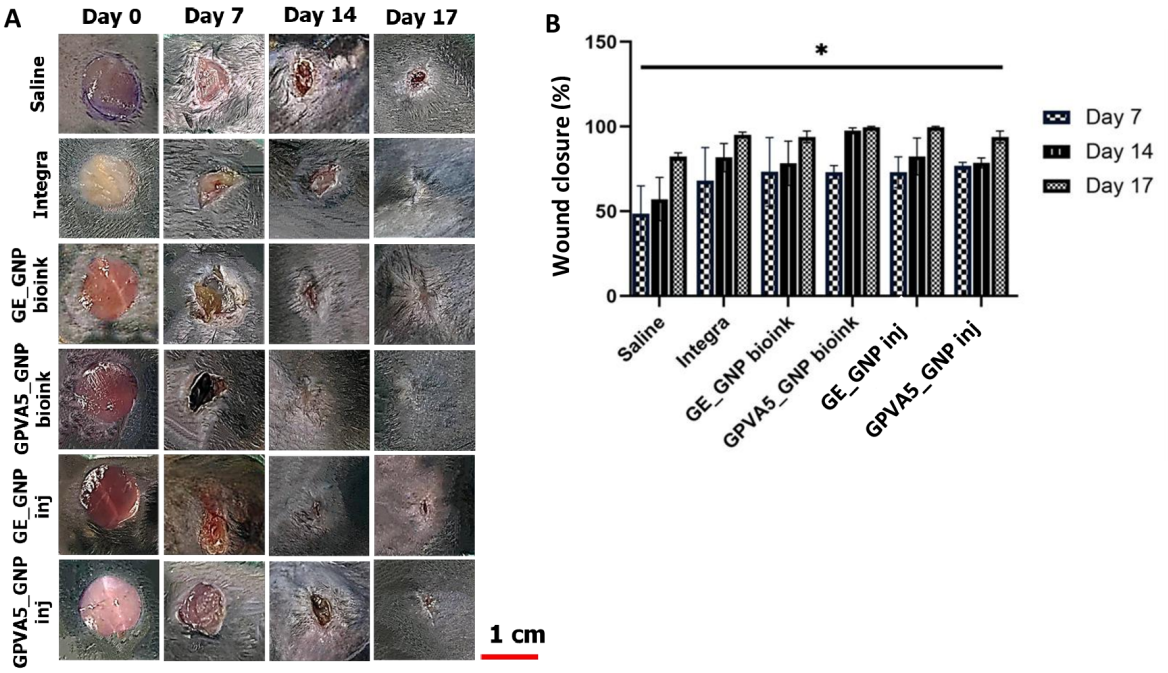

Figure 3. Effect of 3D-bioprinted and injectable hydrogels on wound healing in diabetic C57BL/6 mice. (A) Representative gross images of wound healing at the indicated time points. All wounds were measured on days 0, 7, 14, and 17. (B) Wound closure (%) was calculated as the percentage reduction in wound area relative to the wound area on day 0. Wound closure values are presented as the mean ± standard deviation; *$p < 0.05$. Scale bar: 1 cm.

hydrogels, and Integra groups) compared with the saline group. Histological analysis showed greater granulation tissue formation at the wound sites in the treated groups, with abundant cells. The bioink and injectable hydrogel groups also showed dense collagen fibres. These findings suggest that the bioinks and injectable hydrogels supported wound healing and skin regeneration.

Subsequently, picrosirius red staining was used to assess collagen deposition in newly regenerated skin. Skin contains abundant type I and type III collagens, both of which contribute to extracellular matrix remodelling during wound healing. As shown in Figure 6B, wounds treated with bioinks and injectable hydrogels showed denser and more organised collagen deposition on day 17 than the saline group, indicating that hydrogel treatments promoted collagen I and collagen III production. Moreover, collagen deposition in the GE_GNP bioink and GPVA5_GNP bioink groups appeared denser and more aligned than that in the injectable hydrogel groups.

3.5. Immunofluorescence analysis of newly regenerated skin in diabetic mice

The histological findings were further supported by immunofluorescence analysis. To assess collagen type I and α-SMA expression, the dermal layer of freshly regenerated skin was stained for collagen type I and α-SMA. As shown in Figure 7A, collagen type I was identified in both the treated groups and the saline group. However, collagen type I staining was lower in the saline group than in the treated groups (injectable hydrogel, bioinks, and Integra). In contrast, as shown in Figure 7B, α-SMA staining was more prominent in the saline group than in the treated groups.

Next, the newly formed epidermis was stained for CK14 and involucrin, markers of basal keratinocytes and differentiating keratinocytes, respectively. CK14 is a type I cytokeratin. Generally, cytokeratins are components of the cytoskeleton of epithelial cells and play an important role in maintaining the structural integrity of epithelial tissues, including the skin. Figure 7C shows that CK14 expression in the Integra, GE_GNP bioink, GPVA5_GNP bioink, GE_GNP inj, and GPVA5_GNP inj groups was similar to that in normal skin. This finding indicates the presence of basal keratinocytes at the wound edges during wound healing. These cells play a vital role in re-epithelialisation, during which new epithelial cells cover the wound surface.

In addition, involucrin is a structural protein that becomes crosslinked to other proteins during formation of the cornified envelope in differentiated keratinocytes. As shown in Figure 7D, all groups treated with injectable

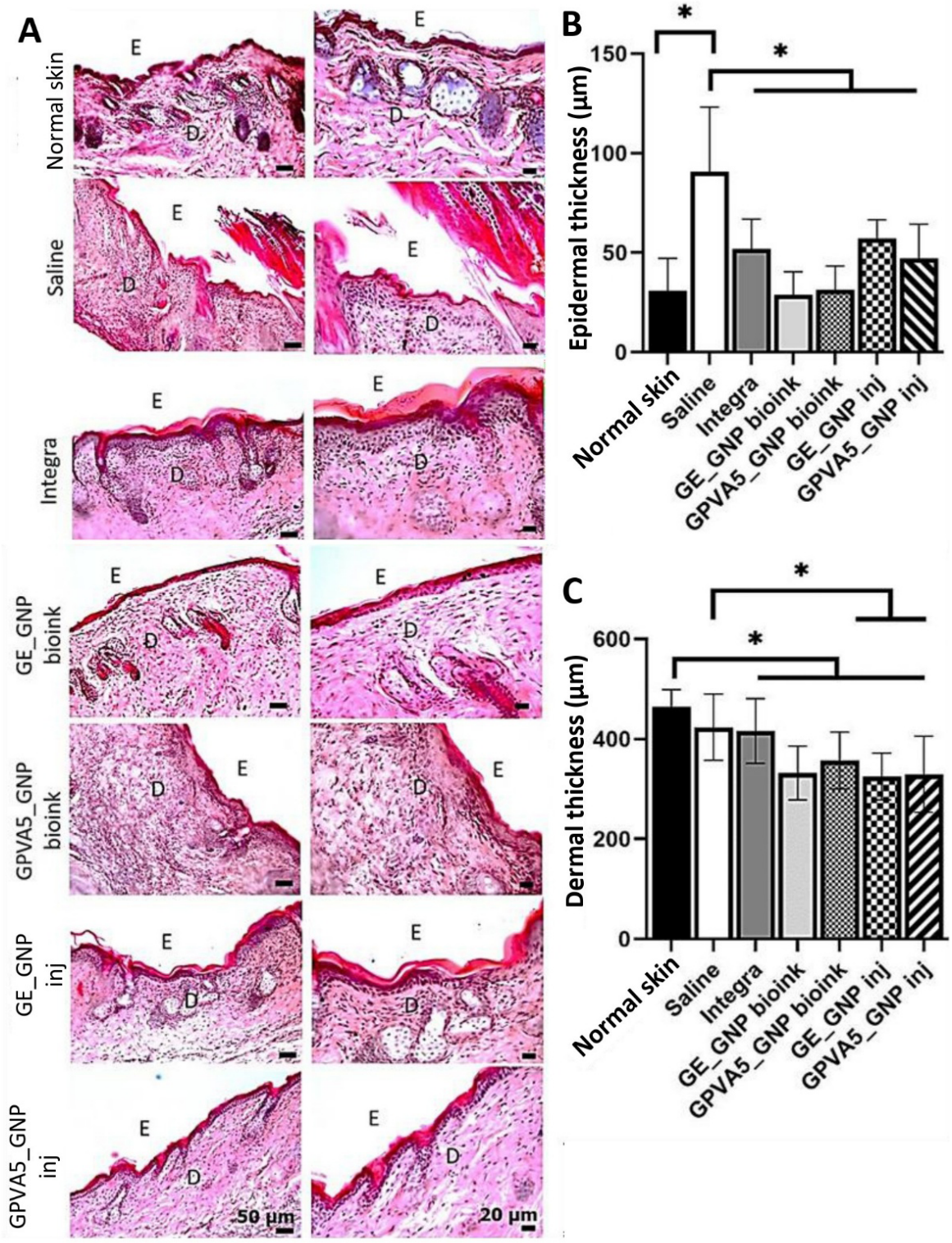

Figure 4. Histological analysis of epidermal and dermal regeneration during wound healing. (A) Hematoxylin and eosin staining. Notes: D: Dermis; E: Epidermis. (B) Quantitative evaluation of epidermal thickness after 17 days of wound healing. (C) Quantitative evaluation of dermal thickness after 17 days of wound healing. Scale bars: 50 µm, magnification: 20×; 20 µm, magnification: 40×. $^{*}p < 0.05$.

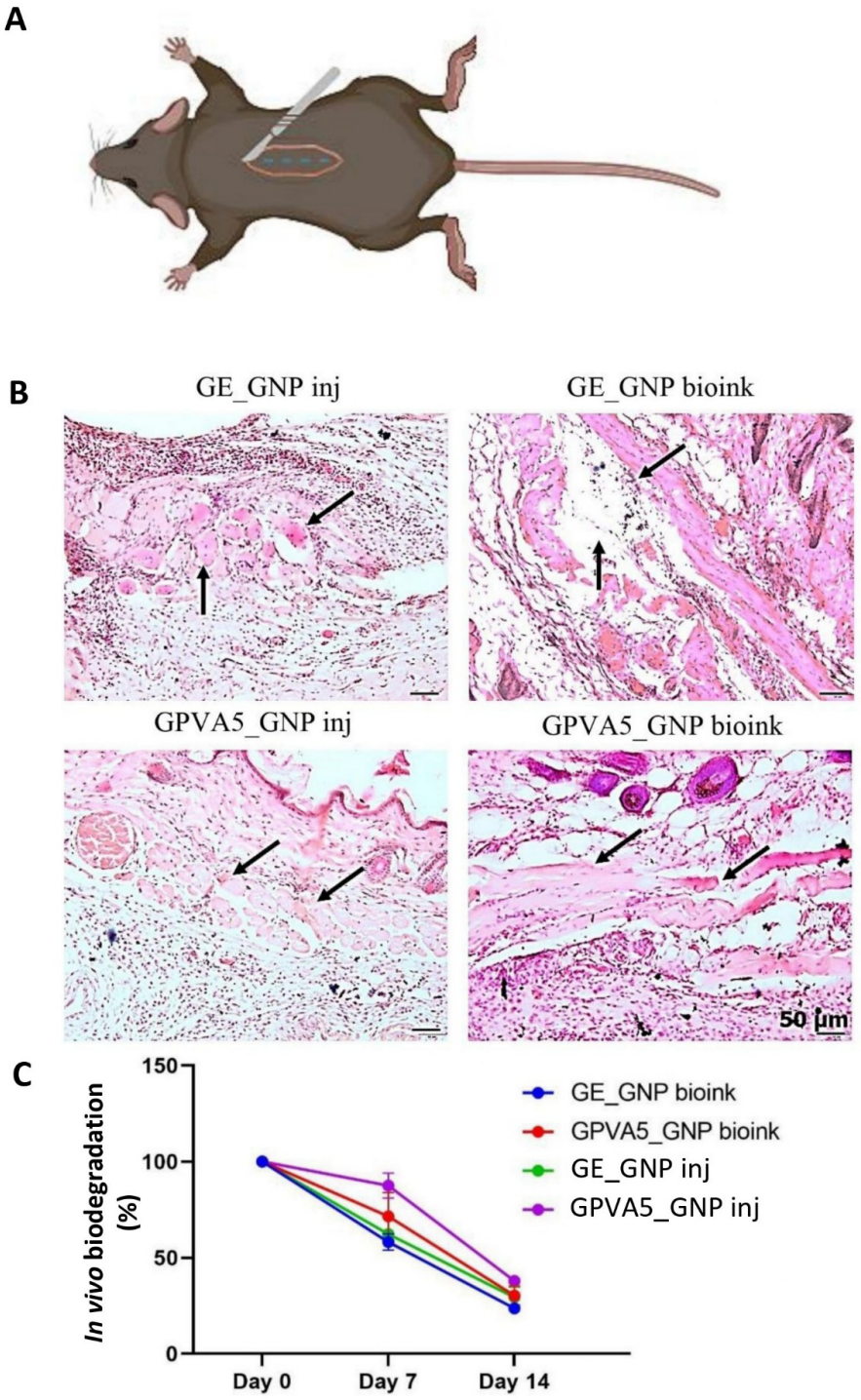

Figure 5. *In vivo* biodegradation and histological evaluation of the implanted bioinks and injectable hydrogels. (A) Illustration of subcutaneous implantation model. Notes: LP: Left pocket; RP: Right pocket. (B) Quantitative *in vivo* biodegradation data (%) on day 0, 7, and 14 for the bioinks and injectable hydrogels. (C) Hematoxylin and eosin staining of subcutaneous skin tissue surrounding the bioinks and injectable hydrogels on day 14. The black arrows indicate hydrogel degradation. Dashed lines indicate the presumed boundary between residual hydrogel and skin tissue. Scale bars: 50 μm; magnification: 200×.

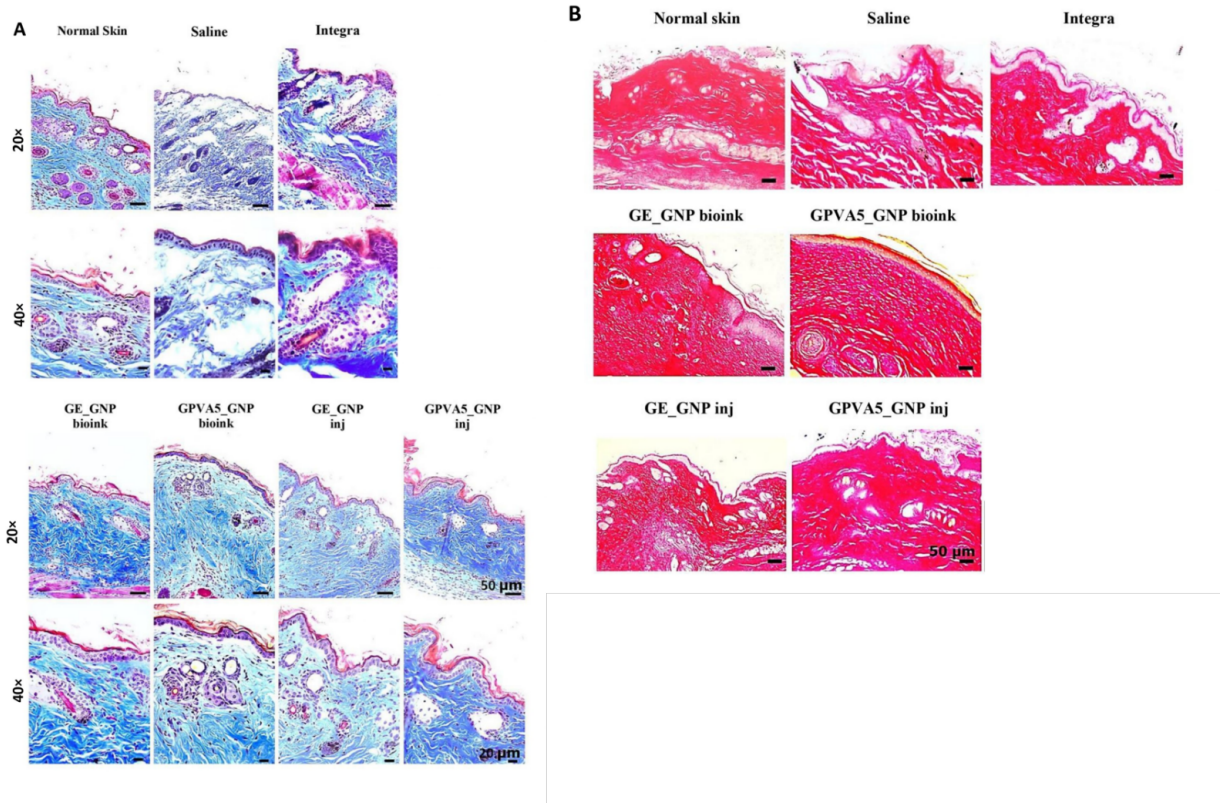

Figure 6. Histological analysis of newly regenerated skin on day 17. (A) Masson's trichrome staining of mouse skin, with collagen stained blue, muscle fibres red, and cytoplasm dark red/blue. Notes: D: Dermis; E: Epidermis. (B) Picrosirius red staining of newly regenerated skin, with collagen stained red and muscle fibres and cytoplasm yellow. Scale bars: 50 µm; magnification: 20×.

hydrogels and bioinks exhibited keratinised cells with positive involucrin staining in the outer epidermal layer. This finding was particularly noticeable in the GE_GNP and GPVA5_GNP bioink groups, the GE_GNP and GPVA5_GNP injectable hydrogel groups, and normal skin. In contrast, the saline group showed no involucrin staining, consistent with ongoing wound healing. During wound healing, involucrin expression increases as keratinocytes differentiate to form the new epithelial layer covering the lesion.

3.6. Transmission electron microscopy of newly regenerated skin (epidermal, dermal–epidermal junction, and dermis)

Transmission electron microscopy was used to examine the ultrastructure of the epidermis, DEJ, and dermis (Figure 8). The treatment groups (bioinks, injectable hydrogels, and Integra) showed tight junctions and keratin intermediate filaments in the epidermal layer, DEJ, and compact collagen fibrils in the dermis that were comparable to those observed in normal skin. Because the dermal layer is rich in collagen, all treated groups showed denser collagen fibrils compared with the saline group, which showed less dense collagen fibrils, indicating that wound healing was still in progress. The collagen fibrils were characterised by alternating dark and light bands with cross-striations. Moreover, establishment of the DEJ is crucial for maintaining skin integrity. The presence of the desmosomes between keratinocytes is used to evaluate epidermal integrity, while the presence of hemidesmosomes is used to evaluate the adhesion of the epidermis to the dermis at the basement membrane. Thus, all treated groups exhibited DEJ formation similar to that observed in normal skin, whereas the saline group showed no evidence of DEJ formation.

4. Discussion

Conventional wound dressings such as bandages and gauze are highly absorbent and useful for dry to lightly exuding wounds. However, they need to be changed regularly, which can cause pain with each dressing change.[19] In addition, their adherence may be inadequate. Consequently, wound healing may be delayed. Therefore, modern skin substitutes have been developed with semipermeable and

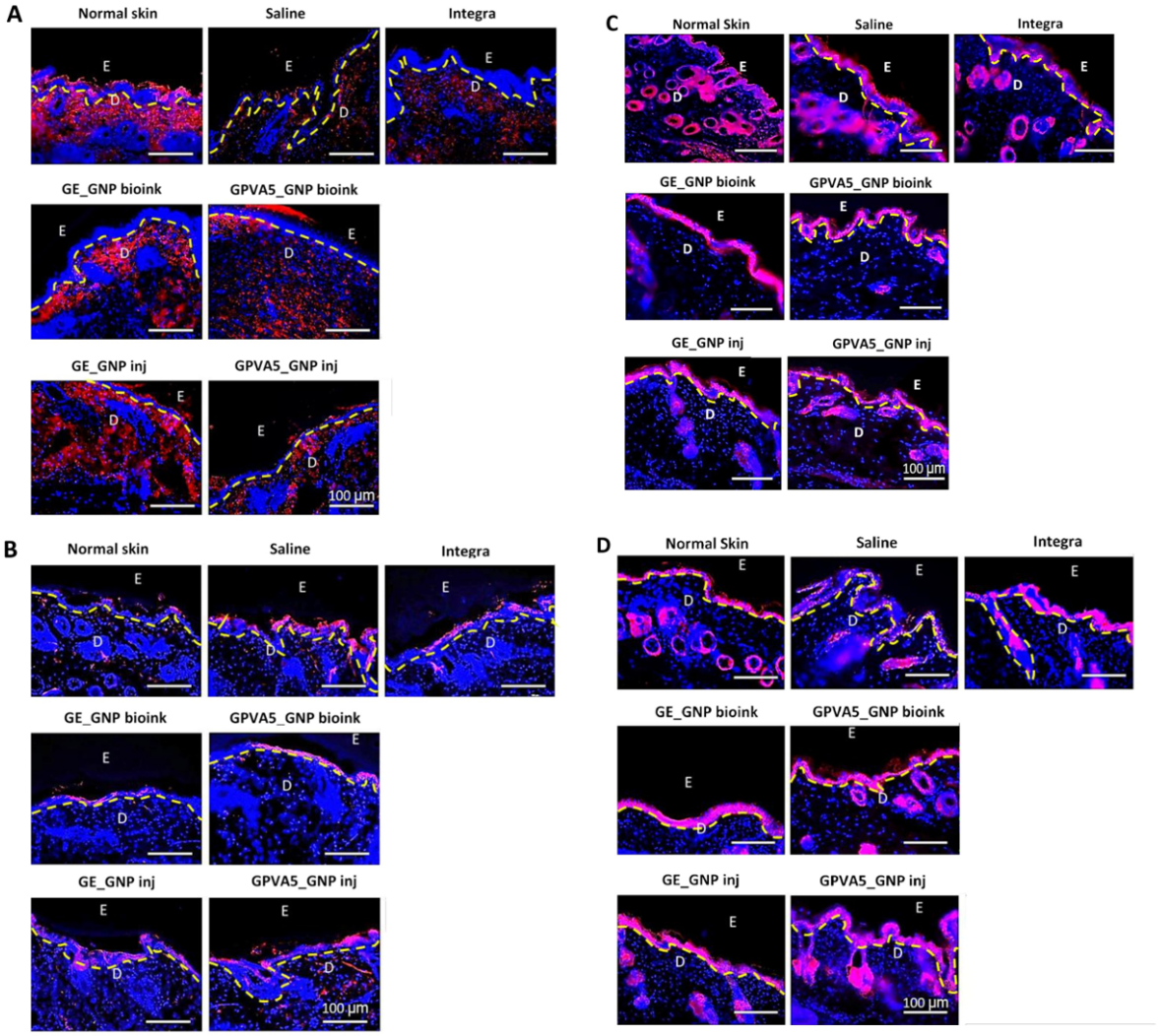

Figure 7. Immunofluorescence staining of mouse skin on day 17. (A) Collagen type I immunostaining, with positive staining shown in red, indicating the presence of collagen type I. (B) Alpha-smooth muscle actin (α-SMA) immunostaining, with α-SMA-positive cells shown in red, indicating the presence of myofibroblasts associated with wound contraction during the wound healing process. (C) Cytokeratin 14 (CK14) staining, with CK14-positive basal keratinocytes shown in red in the epidermal layer of the experimental groups. CK14-positive cells in the epidermis indicate the presence of basal keratinocytes involved in epidermal regeneration. (D) Involucrin immunostaining of the epidermis in the experimental groups. Involucrin-positive cells (red) are visible in the outer epidermal layer of the treated groups. Blue staining indicates nuclei.
Notes: D: Dermis; E: Epidermis. Scale bars: 100 µm; magnification: 100×.

highly absorbent properties. In this study, we utilised two different treatment strategies, 3D-bioprinted cell-laden constructs and cell-free injectable hydrogels, for rapid treatment (6–8 h after biopsy) using GNP-crosslinked GE and GE–PVA with or without encapsulated skin cells as skin substitutes.

In the tissue engineering field, 3D-bioprinting is an advanced technology that has the capacity to enhance wound healing and tissue regeneration through the use of bioinks. Generally, 3D bioprinting allows precise control of cell dispersion within 3D structures, thereby improving cell–cell and cell–matrix interactions.[11] Mouse skin cells were isolated and encapsulated in the corresponding hydrogels to form the GE_GNP and GPVA5_GNP bioinks. The 0.1% GNP concentration was selected based on our previous optimisation study, which demonstrated an appropriate balance between hydrogel crosslinking and biological compatibility.[1,16] An advantage of the 3D-bioprinting technique is that it facilitates the precise positioning of skin cells to repair damaged skin.[20]

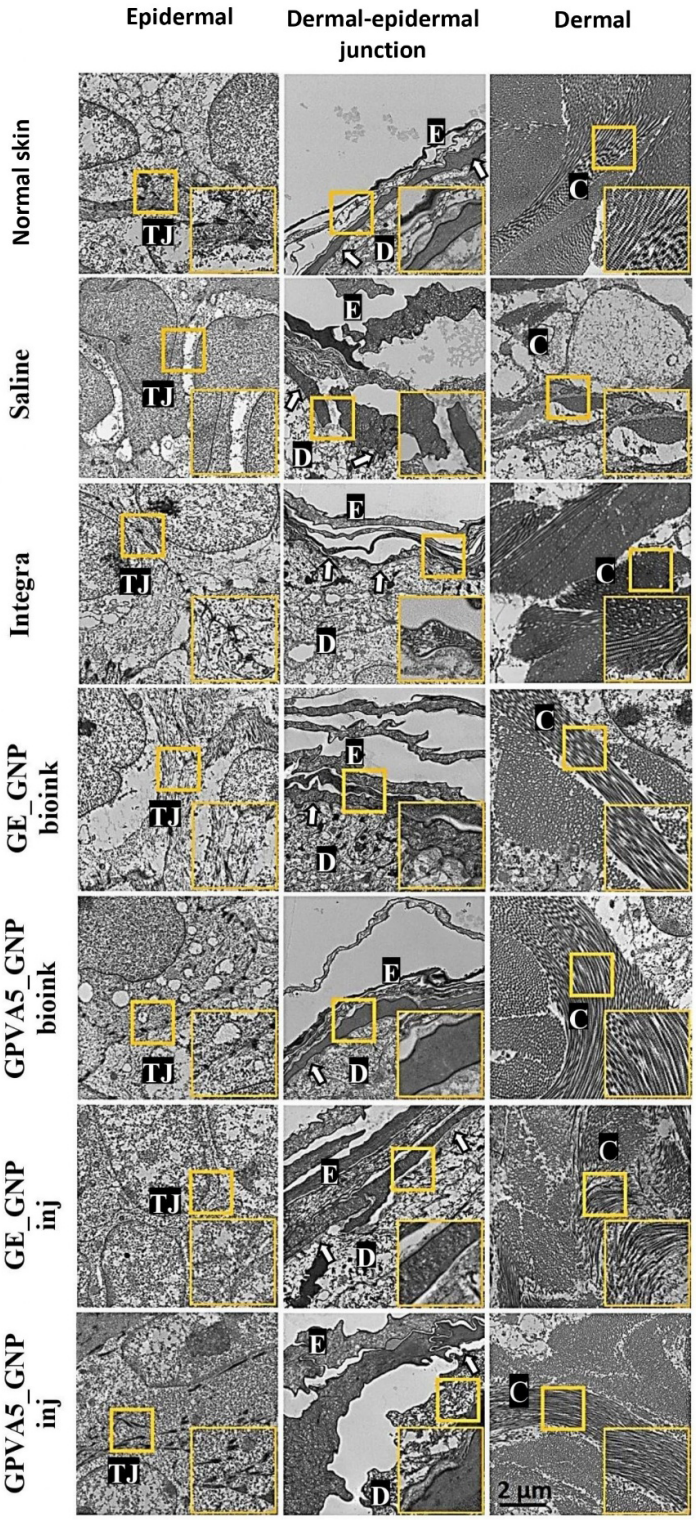

Figure 8. Transmission electron micrographs of the epidermis, dermal–epidermal junction, and dermis in normal skin and the saline, Integra, bioink, and injectable hydrogel groups.

Notes: C: Collagen fibres; D: Dermis; E: Epidermis; TJ: Tight junction. Yellow boxes indicate the regions of interest shown at higher magnification in the corresponding insets. Scale bar: 2 μm; magnification: 5,300×.

In our previous studies,[1,15,16] the biocompatibility of both bioinks and injectable hydrogels (GE_GNP bioink, GPVA5_GNP bioink, GE_GNP inj, and GPVA5_GNP inj) was examined, revealing that both formulation types promoted the adhesion and growth of skin cells. Moreover, the biocompatibility of the GE_GNP and GPVA5_GNP hydrogels has been established in our previous studies using human dermal fibroblasts.[1,15,16]

In the present study, PBMC metabolic activity was initially higher after 24 h of culture with the hydrogels and gradually decreased over time. This observation may reflect the early interaction between PBMCs and the hydrogels. Following biomaterial implantation, immune cells are naturally recruited to the implantation site and interact with the foreign material as part of the host response, facilitating tissue remodelling and material degradation.[21]

Diabetes is a chronic disease characterised by elevated blood glucose levels, known as hyperglycemia.[22] Diabetes impairs wound healing, which may be further compromised by diabetic complications. Animal models currently play a crucial role in studies of chronic wound healing. Consequently, the efficacy of skin substitutes, including bioinks and injectable hydrogels, in promoting rapid wound healing was evaluated in a C57BL/6 mouse model. The skin cells used in this study were obtained from a skin biopsy (1 cm^2) and subsequently combined with the corresponding hydrogels to form the GE_GNP and GPVA5_GNP bioinks. According to a previous study, scaffolds containing skin cells have been hypothesised to accelerate the healing process.[14] However, no previous research has evaluated the efficacy of skin cells encapsulated in GE–PVA-based bioinks in a diabetic mouse wound-healing model. In the present study, the bioink groups showed more advanced re-epithelialisation of diabetic wounds by day 17, followed by the injectable hydrogel and Integra group. The absence of crusts on the newly formed skin in the bioink groups suggested more advanced wound healing.

Furthermore, compared with the injectable hydrogel and Integra groups, both the GE_GNP and GPVA5_GNP bioink groups exhibited minimal contraction on gross observation. Although a non-splinted wound model was used in the present study, this approach was consistent with a previous study in which wound contraction was minimised by selecting the hind-leg/thigh region.[23] Nevertheless, wound contraction may still have contributed to the observed wound closure in mice. Therefore, future studies using a splinted wound model are recommended to further distinguish wound contraction from tissue regeneration. In addition, the lower α-SMA expression observed in the bioink groups may indicate reduced myofibroblast activation, which could contribute to controlled wound contraction and tissue remodelling. This characteristic may help reduce excessive contraction and scar formation during the healing process. The controlled myofibroblast response may also support balanced extracellular matrix deposition during the later stages of wound healing.

Compared with the treated groups, the untreated saline group demonstrated slower healing on day 17, including the formation of a scar and scab. No previous study has evaluated the efficacy of GE–PVA bioinks containing encapsulated skin cells in a diabetic mouse model. For comparison, a previous study evaluated gelatin methacryloyl bioink in diabetic mice and reported complete wound healing by day 21.[24] The present findings demonstrate that both the cell-laden bioinks and acellular injectable hydrogels effectively promoted wound healing within 17 days. While comparable wound closure was achieved, the incorporation of freshly isolated skin cells primarily enhanced the structural maturation of the regenerated skin, as evidenced by improved epidermal organisation, DEJ formation, collagen remodelling, and skin-specific protein expression.

Moreover, effective wound treatment requires an appropriate biodegradation rate accompanied by new tissue regeneration. In this study, the *in vivo* biodegradation results demonstrated that the bioinks degraded faster than the injectable hydrogels. Similarly, the 3D-bioprinted hydrogels exhibited a faster degradation rate than the injectable hydrogels when subjected to enzymatic degradation *in vitro*. Nevertheless, the biodegradation rate was substantially slower *in vivo* than *in vitro*. These findings suggest that the biodegradation characteristics of the formulations were compatible with tissue regeneration during the 17-day wound-healing period.

Although the present study demonstrates the feasibility of completing bioink preparation, bioprinting, and implantation within 6–8 h following skin biopsy for autologous cell isolation, several challenges should be considered before clinical translation. Freshly isolated skin cells comprise a heterogeneous population, including fibroblasts, keratinocytes, endothelial cells, and other resident skin cells, which may respond differently to the extrusion-based bioprinting process. Nevertheless, our previous optimisation study demonstrated that the optimised GE–PVA bioinks maintained high post-printing cell viability (>90%), indicating that the selected rheological properties and printing conditions minimised shear-induced cellular damage during extrusion.[16] Furthermore, successful clinical implementation will require a standardised aseptic workflow for cell isolation, bioink

preparation, and bioprinting to ensure reproducibility and patient safety. Therefore, the proposed strategy should be regarded as a preclinical proof-of-concept demonstrating the feasibility of a rapid autologous bioprinting approach, while further translational studies are warranted before routine clinical application.

Furthermore, the maturity and integrity of the regenerated skin also play a role in determining the effectiveness of wound healing. H&E staining demonstrated a higher degree of wound re-epithelisation in the bioinks and injectable hydrogel groups than in the untreated group. The epidermis in the Integra group was thick and stratified, with prominent rete-ridge projections into the dermis compared to the other groups. Meanwhile, normal skin exhibited a thin epidermal layer similar to that observed in the bioink groups. Compared with the granulation tissue observed in the saline and injectable hydrogel groups, wound histology revealed that the bioink groups had the most robust epidermal covering at the centre of the wound. In addition, all treatment groups exhibited increased cellularity compared with normal tissue, indicating an augmentation of inflammatory cells in the region of the healing lesion. Wounds treated with injectable hydrogels appeared to have an immature epidermis that lacked rete-ridge projections into the dermis. Dermal regeneration is important for wound re-epithelialisation and keratinocyte migration.[25] Keratinocyte migration from the wound edges is necessary for wound re-epithelisation. The interactions among keratinocytes, dermal fibroblasts, and the extracellular matrix influence keratinocyte migration and proliferation during this phase.

Furthermore, the developed GE–PVA–GNP hydrogels may have the potential to support wound-bed reinnervation. Previous studies have reported that GE-based hydrogels can support Schwann cell viability and proliferation, neurite extension, and glial cell recruitment, while GE–PVA systems may enhance Schwann cell recruitment and adhesion.[26] However, this potential was not directly evaluated in the present study and requires further investigation.

Collagen is the major component of the 3D dermal extracellular matrix, which also contains glycosaminoglycans, proteoglycans, laminin, fibronectin, elastin, and other cellular components. Hyperglycemia can alter collagen synthesis by increasing collagen crosslinking and inducing nonenzymatic glycation of collagen. This can lead to the formation of aberrant and inflexible collagen fibres and impair the quality of granulation tissue within the wound. The histological findings were further demonstrated by Masson's trichrome and picrosirius red staining, which showed enhanced extracellular matrix deposition and collagen organisation within the regenerated dermis of the treated wounds. In Masson's trichrome staining, healthy skin exhibited intense blue collagen staining in the dermis and red cytoplasmic staining in the epidermis. Similarly, the treated groups demonstrated abundant collagen deposition throughout the dermal layer together with increased cellularity in both the epidermis and dermis, indicating active tissue remodelling during wound healing. These findings are consistent with the study by Jorgensen *et al.*,[27] who reported increased collagen deposition in wounds treated with bioprinted hydrogels. Furthermore, picrosirius red staining revealed a more homogeneous distribution and compact arrangement of collagen fibres within the regenerated dermis of the treated groups compared with the saline-treated control, suggesting progressive restoration of the dermal extracellular matrix architecture during the remodelling phase.

Histological and electron microscopy analyses showed that all treated groups developed more mature epidermal and dermal structures after 17 days than the untreated group. Development of the DEJ is crucial for the stability and integrity of regenerated skin in both the epidermis and dermis.[14] Histologically, DEJ development was reflected by the formation of small rete ridges in the basal epidermal layer. TEM revealed clearly defined electron-lucent lamina lucida and electron-dense lamina densa, which are characteristic components of the DEJ. Moreover, the presence of desmosomes in electron micrographs of the treated groups indicated the establishment of cell–cell junctions in the epidermis. In addition, TEM demonstrated collagen fibrils in the dermal layer of the newly regenerated skin in all treated groups.

Overall, there was no significant difference in wound-healing outcomes between the bioinks and injectable hydrogel groups. Nevertheless, the cell-laden bioinks exhibited enhanced remodelling of the newly regenerated skin, as demonstrated by histological evaluation and protein expression. During remodelling, the extracellular matrix is reorganised, degraded, and resynthesised to maximise tensile strength.[28] In the bioink groups containing skin cells, extracellular matrix deposition, particularly collagen deposition, was more abundant and better organised than that observed in the injectable hydrogel groups. Briefly, encapsulation of skin cells within the bioinks may have supported tissue regeneration through cell proliferation and interactions with neighbouring and host cells.

5. Conclusion and future perspective

In conclusion, *in vivo* analyses based on gross appearance, histological and immunofluorescence assessments, and TEM showed that the bioinks and injectable hydrogels

promoted wound healing compared with the saline group. Gross appearance and Masson's trichrome staining revealed that the GE_GNP and GPVA5_GNP bioink groups had more advanced wound healing than the injectable hydrogel groups. Because this treatment strategy utilises freshly isolated cells obtained from a skin biopsy, the resulting bioink construct can be prepared and implanted within 6–8 h after biopsy. Moreover, acellular injectable hydrogels also promoted rapid wound healing in the diabetic mouse model. Therefore, injectable hydrogels without skin cells may potentially be employed as a rapid treatment approach. Overall, rapid treatment using bioinks containing freshly isolated skin cells or acellular injectable hydrogels shows promise as a potential approach for chronic wounds, with potential relevance to the treatment of DFUs. Furthermore, the reduced production time may offer practical advantages over other autologous tissue-engineered skin substitutes.

Acknowledgments

All authors would like to express immense gratitude to the Faculty of Medicine, UKM, for the guidance and resources to complete this manuscript. This study was conducted under the ISO 9001:2015 standard for research facilities.

Funding

The study was funded by DANA IMPAK PERDANA 2.0 (DIP 2.0) grant under Universiti Kebangsaan Malaysia (grant code: DIP-2023-018).

Conflict of interest

Mh Busra Fauzi is an Editorial Board Member of this journal, but was not in any way involved in the editorial and peer-review process conducted for this paper, directly or indirectly. The authors declare no conflicts of interest.

Author contributions

Conceptualization: All authors
Formal analysis: Syafira Masri, Mh Busra Fauzi, Manira Maarof
Investigation: Syafira Masri, Mh Busra Fauzi
Methodology: All authors
Writing–original draft: Syafira Masri
Writing–review & editing: All authors

Ethics approval and consent to participate

The study design was approved by the Research Ethics Committee of Universiti Kebangsaan Malaysia (Code Nos. FF-2021-376 and JEP-2021-605). The research was conducted at the Department of Tissue Engineering and Regenerative Medicine (DTERM), Faculty of Medicine, Universiti Kebangsaan Malaysia, under an ISO 9001:2015-certified quality management system.

Consent for publication

Not applicable.

Availability of data

Additional data supporting the findings of this study are available from the corresponding author upon reasonable request. Detailed compositional information regarding the bioink and hydrogel formulations is not publicly disclosed due to intellectual property and confidentiality considerations.

References

1. Masri S, Maarof M, Aziz IA, Idrus R, Fauzi MB. Performance of hybrid gelatin-PVA bioinks integrated with genipin through extrusion-based 3D bioprinting: an in vitro evaluation using human dermal fibroblasts. *Int J Bioprint*. 2023;9(3):677.

   doi: 10.18063/ijb.677

2. Eriksson E, Liu PY, Schultz GS, *et al*. Chronic wounds: treatment consensus. *Wound Repair Regen*. 2022;30(2):156-171.

   doi: 10.1111/wrr.12994

3. Atkin L. Chronic wounds: the challenges of appropriate management. *Br J Community Nurs*. 2019;24(Sup9):S26.

   doi: 10.12968/bjcn.2019.24.Sup9.S26

4. Shi C, Wang C, Liu H, *et al*. Selection of appropriate wound dressing for various wounds. *Front Bioeng Biotechnol*. 2020;8:182.

   doi: 10.3389/fbioe.2020.00182

5. Edmonds M, Manu C, Vas P. The current burden of diabetic foot disease. *J Clin Orthop Trauma*. 2021;17:88-93.

   doi: 10.1016/j.jcot.2021.01.017

6. Lin C, Liu J, Sun H. Risk factors for lower extremity amputation in patients with diabetic foot ulcers: a meta-analysis. *PLoS One*. 2020;15(9):e0239236.

   doi: 10.1371/journal.pone.0239236

7. Boulton AJM. The 2017 Banting Memorial Lecture The diabetic lower limb - a forty year journey: from clinical observation to clinical science. *Diabet Med*. 2019;36(12):1539-1549.

   doi: 10.1111/dme.13901

8. Glover K, Stratakos AC, Varadi A, Lamprou DA. 3D scaffolds in the treatment of diabetic foot ulcers: new trends vs conventional approaches. *Int J Pharm*. 2021;599:120423.

   doi: 10.1016/j.ijpharm.2021.120423

9. Güiza-Argüello VR, Solarte-David VA, Pinzón-Mora AV, Ávila-Quiroga JE, Becerra-Bayona SM. Current advances in the development of hydrogel-based wound dressings for diabetic foot ulcer treatment. *Polymers (Basel)*. 2022;14(14):2764.

   doi: 10.3390/polym14142764

10. Fayyazbakhsh F, Leu MC. A brief review on 3D bioprinted skin substitutes. *Procedia Manuf*. 2020;48:790-796.

    doi: 10.1016/j.promfg.2020.05.115

11. He P, Zhao J, Zhang J, *et al*. Bioprinting of skin constructs for wound healing. *Burns Trauma*. 2018;6:5.

    doi: 10.1186/s41038-017-0104-x

12. Ng WL, Bartolo P. 3D bioprinting of tissues and organs for systemic diseases and localized injuries. *Mil Med Res*. 2026;13(1):100006.

    doi: 10.1016/j.mmr.2026.100006

13. Chouhan D, Dey N, Bhardwaj N, Mandal BB. Emerging and innovative approaches for wound healing and skin regeneration: current status and advances. *Biomaterials*. 2019;216:119267.

    doi: 10.1016/j.biomaterials.2019.119267

14. Busra FM, Lokanathan Y, Mohd Nadzir M, Saim A, Hj Idrus R, Chowdhury SR. Attachment, Proliferation, and Morphological Properties of Human Dermal Fibroblasts on Ovine Tendon Collagen Scaffolds: A Comparative Study. *Malays J Med Sci*. 2017;24(2):33-43.

    doi: 10.21315/mjms2016.24.2.5

15. Masri S, Maarof M, Mohd NF, Hiraoka Y, Tabata Y, Fauzi MB. Injectable crosslinked genipin hybrid gelatin-PVA hydrogels for future use as bioinks in expediting cutaneous healing capacity: physicochemical characterisation and cytotoxicity evaluation. *Biomedicines*. 2022;10(10):2651.

    doi: 10.3390/biomedicines10102651

16. Masri S, Md Fadilah NI, Hao LQ, *et al*. Multifunctionalised skin substitute of hybrid gelatin-polyvinyl alcohol bioinks for chronic wound: injectable vs. 3D bioprinting. *Drug Deliv Transl Res*. 2024;14(4):1005-1027.

    doi: 10.1007/s13346-023-01447-z

17. Kitada M, Ogura Y, Koya D. Rodent models of diabetic nephropathy: their utility and limitations. *Int J Nephrol Renovasc Dis*. 2016;9:279-290.

    doi: 10.2147/IJNRD.S103784

18. Furman BL. Streptozotocin-induced diabetic models in mice and rats. *Curr Protoc Pharmacol*. 2015;70:5.47.1-5.47.20.

    doi: 10.1002/0471141755.ph0547s70

19. Brumberg V, Astrelina T, Malivanova T, Samoilov A. Modern wound dressings: hydrogel dressings. *Biomedicines*. 2021;9(9):1235.

    doi: 10.3390/biomedicines9091235

20. Javaid M, Haleem A. 3D bioprinting applications for the printing of skin: a brief study. *Sensors Int*. 2021;2:100123.

    doi: 10.1016/j.sintl.2021.100123

21. Carnicer-Lombarte A, Chen ST, Malliaras GG, Barone DG. Foreign body reaction to implanted biomaterials and its impact in nerve neuroprosthetics. *Front Bioeng Biotechnol*. 2021;9:622524.

    doi: 10.3389/fbioe.2021.622524

22. Rai V, Moellmer R, Agrawal DK. Clinically relevant experimental rodent models of diabetic foot ulcer. *Mol Cell Biochem*. 2022;477(4):1239-1247.

    doi: 10.1007/s11010-022-04372-w

23. Mh Busra F, Rajab NF, Tabata Y, Saim AB, Idrus RBH, Chowdhury SR. Rapid treatment of full-thickness skin loss using ovine tendon collagen type I scaffold with skin cells. *J Tissue Eng Regen Med*. 2019;13(5):874-891.

    doi: 10.1002/term.2842

24. Xia S, Weng T, Jin R, *et al*. Curcumin-incorporated 3D bioprinting gelatin methacryloyl hydrogel reduces reactive oxygen species-induced adipose-derived stem cell apoptosis and improves implanting survival in diabetic wounds. *Burns Trauma*. 2022;10:tkac001.

    doi: 10.1093/burnst/tkac001

25. Rousselle P, Braye F, Dayan G. Re-epithelialization of adult skin wounds: cellular mechanisms and therapeutic strategies. *Adv Drug Deliv Rev*. 2019;146:344-365.

    doi: 10.1016/j.addr.2018.06.019

26. Jia S, Zhou H, Chen J, *et al*. A comprehensive review of hydrogel strategies for repairing peripheral nerve injuries. *Brain-X*. 2025;3(4):e70012.

    doi: 10.1002/brx2.70012

27. Jorgensen AM, Varkey M, Gorkun A, *et al*. Bioprinted skin recapitulates normal collagen remodeling in full-thickness wounds. *Tissue Eng Part A*. 2020;26(9-10):512-526.

    doi: 10.1089/ten.TEA.2019.0319

28. Gonzalez ACO, Costa TF, Andrade ZA, Medrado ARAP. Wound healing - a literature review. *An Bras Dermatol*. 2016;91(5):614-620.

    doi: 10.1590/abd1806-4841.20164741